Published in final edited form as:
Cortex. 2014 September ; 58: 72–85. doi:10.1016/j.cortex.2014.04.018.

Disruption of response inhibition circuits in prodromal Huntington disease

Julia A. Rao[a], **Deborah L. Harrington**[b,c], **Sally Durgerian**[d], **Christine Reece**[e], **Lyla Mourany**[e], **Katherine Koenig**[f], **Mark J. Lowe**[f], **Vincent A. Magnotta**[g], **Jeffrey D. Long**[g], **Hans J. Johnson**[g], **Jane S. Paulsen**[g,**], and **Stephen M. Rao**[e,*]

[a] Department of Psychiatry, University of Illinois at Chicago, Chicago, IL, USA

[b]*VA San Diego Healthcare System, San Diego, CA, USA*

[c] Department of Radiology, University of California, San Diego, La Jolla, CA, USA

[d] Department of Neurology, Medical College of Wisconsin, Milwaukee, WI, USA

[e] Schey Center for Cognitive Neuroimaging, Neurological Institute, Cleveland Clinic, Cleveland, OH, USA

[f] Imaging Institute, Cleveland Clinic, Cleveland, OH, USA

[g] Carver College of Medicine, The University of Iowa, Iowa City, IA, USA

Abstract

Cognitive changes in the prodromal phase of Huntington disease (prHD) are found in multiple domains, yet their neural bases are not well understood. One component process that supports cognition is inhibitory control. In the present fMRI study, we examined brain circuits involved in response inhibition in 65 prHD participants and 36 gene-negative (NEG) controls using the stop signal task (SST). PrHD participants were subdivided into three groups (LOW, MEDIUM, HIGH) based on their CAG-Age Product (CAP) score, an index of genetic exposure and a proxy for expected time to diagnosis. Poorer response inhibition (stop signal duration) correlated with CAP scores. When response inhibition was successful, activation of the classic frontal inhibitory-network was normal in prHD, yet stepwise reductions in activation with proximity to diagnosis were found in the posterior ventral attention network (inferior parietal and temporal cortices). Failures in response inhibition in prHD were related to changes in inhibition centers (supplementary motor area (SMA)/anterior cingulate and inferior frontal cortex/insula) and ventral attention networks, where activation decreased with proximity to diagnosis. The LOW group showed evidence of early compensatory activation (hyperactivation) of right-hemisphere inhibition and attention reorienting centers, despite an absence of cortical atrophy or deficits on

[*]*Corresponding author*. Schey Center for Cognitive Neuroimaging, Neurological Institute, Cleveland Clinic, 9500 Euclid Avenue/ U10, Cleveland, OH 44195, USA. raos2@ccf.org (S.M. Rao). [**]*Corresponding author*. Department of Psychiatry, University of Iowa Carver College of Medicine, 1-305 Medical Education Building, Iowa City, IA 52242, USA. jane-paulsen@uiowa.edu (J.S. Paulsen)..

Competing interests
None declared.

Supplementary data
Supplementary data related to this article can be found at http://dx.doi.org/10.1016/j.cortex.2014.04.018.

tests of executive functioning. Moreover, greater activation for failed than successful inhibitions in an ipsilateral motor-control network was found in the control group, whereas such differences were markedly attenuated in all prHD groups. The results were not related to changes in cortical volume and thickness, which did not differ among the groups. However, greater hypoactivation of classic right-hemisphere inhibition centers [inferior frontal gyrus (IFG)/insula, SMA/anterior cingulate cortex (ACC)] during inhibition failures correlated with greater globus pallidus atrophy. These results are the first to demonstrate that response inhibition in prHD is associated with altered functioning in brain networks that govern inhibition, attention, and motor control.

Keywords

fMRI; Response inhibition; Huntington's disease; Brain activation; Brain atrophy; Neuropsychological testing

1. Introduction

Huntington disease (HD) is an autosomal dominant neurode-generative disorder characterized by the gradual onset and progression of motor, cognitive, and psychiatric symptoms. HD is caused by a cytosine-adenine-guanine (CAG) triplet repeat expansion in the huntingtin (HTT) gene. Longer CAG repeat lengths predict earlier ages of HD onset (Andresen et al., 2007; Duyao et al., 1993), the diagnosis of which is based on the presence of unequivocal extrapyramidal motor signs of chorea, dystonia, bradykinesia, or incoordination (HSG, 1996). HD affects the whole brain, but the most prominent early effect is characterized by a loss of small to medium spiny neurons in the caudate and putamen (Vonsattel & DiFiglia, 1998). However, other neuropathology (e.g., corticostriatal gray-matter atrophy, white-matter volume loss) and subtle signs of the disease, including cognitive changes, are seen during the prodromal HD (prHD) phase, decades prior to the diagnosis of manifest HD (Duff et al., 2010; Harrington, Smith, Zhang, Carlozzi, & Paulsen, 2012; Nopoulos et al., 2010; Novak et al., 2012; Paulsen et al., 2006; Paulsen et al., 2008; Paulsen et al., 2001; Rosas et al., 2005). In conjunction with efforts to identify efficacious treatments to slow disease progression, there has been a concerted effort to identify neuroimaging biomarkers of early brain changes that could serve as outcomes in primary prevention trials of individuals in the prHD phase, when treatments are more likely to succeed.

Subtle cognitive changes in prHD have been reported in many domains, including attention, working memory, and various executive functions (Duff et al., 2010; Georgiou-Karistianis et al., 2012; Harrington et al., 2012; O'Rourke et al., 2011; Paulsen et al., 2008; Stout et al., 2011). Yet the brain mechanisms that govern different facets of cognitive decline in prHD are not well understood. Emerging functional imaging studies report different disease-related patterns of activation during working memory (Wolf et al., 2008; Wolf, Vasic, Schonfeldt-Lecuona, Landwehrmeyer, & Ecker, 2007), attention (Wolf et al., 2012), interference (Reading et al., 2004), temporal processing (Paulsen et al., 2004; Zimbelman et al., 2007), set shifting (Gray et al., 2013), and implicit emotion processing (Novak et al., 2012), typically without deficits in task performance. Some studies report changes in brain

functioning in individuals far from a diagnosis (Paulsen et al., 2004; Wolf et al., 2007; Zimbelman et al., 2007), despite the absence of cognitive decline and/or striatal atrophy. This suggests that fMRI may be sensitive to the earliest prodromal changes in brain networks. It is therefore important to elucidate functional changes associated with different facets of cognition, especially given the heterogeneity of cognitive phenotypes in prHD (Duff et al., 2010).

One core component process that supports cognition is inhibitory control, which is thought to be governed by functionally distinct, but partially overlapping networks. The classic inhibition network is comprised of the right inferior frontal gyrus (IFG), anterior insula, supplementary motor area (SMA), superior frontal gyrus, and structures of the basal ganglia (Aron & Poldrack, 2006). However, recent research suggests that more distributed bilateral networks also expedite inhibitory control, including elements of the ventral attention network (insula, temporal and inferior parietal cortices) that reorient attention to task-relevant events, error processing systems (midline basal ganglia-thalamocortical), and motor-control centers (precentral and postcentral gyrus; SMA, cerebellum) that regulate motor preparation and execution (Boehler, Appelbaum, Krebs, Hopf, & Woldorff, 2010; Hampshire, Chamberlain, Monti, Duncan, & Owen, 2010; Zhang & Li, 2012). Inhibitory control is impaired in manifest HD on a variety of tasks (Aron et al., 2003; Beste, Saft, Andrich, Gold, & Falkenstein, 2008; Henderson et al., 2011; Swerdlow et al., 1995) and in prHD (Beste, Willemssen, Saft, & Falkenstein, 2010; Majid, Cai, Corey-Bloom, & Aron, 2013). Although the sources of impairment are not well understood, event-related potential (ERP) recordings in prHD during response inhibition demonstrated weakened medial-frontal (FCz electrode) N2 delta-band power and phase-locking (Beste, Ness, Falkenstein, & Saft, 2011) and P3 amplitudes (Beste et al., 2010), but the analyses did not separate successful and unsuccessful inhibition trails. There is also evidence of diminished inhibitory control in prHD on neuropsychological tests of switching (e.g., Trail Making Test) and Stroop interference (O'Rourke et al., 2011; Stout et al., 2011), but their neural underpinnings are not known.

The present fMRI study investigated the brain mechanisms that govern inhibitory control in a large cohort of gene-positive prHD participants (n = 65) and gene-negative controls (n = 36). We used the stop signal task (SST) (Aron & Poldrack, 2006), which tests the ability to inhibit a prepotent response that is already started. In the SST, go and stop trials are presented in a 3:1 ratio, which establishes a prepotent response to the go stimulus. On stop trials, task accuracy is maintained at 50% by adjusting the time between the go and the stop stimulus (i.e., stop signal duration) based on previous trial performances. Shorter stop signal durations are indicative of poorer control over inhibiting a prepotent response that is about to be executed. This procedure allows for an analysis of successful and unsuccessful stop trials, which differ in their engagement of some brain networks (Zhang & Li, 2012), unlike the Go-NoGo task (Beste et al., 2011, 2008, 2010). Activation associated with inhibition successes and failures (relative to go trials) both should reveal prHD abnormalities in some of the same inhibition networks. However, disturbances in systems that govern successful response inhibition may also correlate with the proficiency of inhibitory control (SSD). In contrast, failures in response inhibition might be associated with disturbances in multiple

processes and therefore, found in many systems including classic inhibition, ventral attention, motor control, and error processing centers.

We first sought to determine whether the prHD group demonstrated deficits in SST performance and altered brain activation relative to controls. Then we examined the relationship between a surrogate measure of proximity to diagnosis and neurocognition. This was accomplished by stratifying prHD individuals into three groups (LOW, MEDIUM, HIGH) based on an index of baseline genetic exposure, the CAG-Age Product (CAP) score, which is a proxy for time to diagnosis (Zhang et al., 2011). Based on earlier research, we predicted that individuals with a low probability of diagnosis would exhibit hyperactivation in some brain regions relative to controls and participants with a high probability of diagnosis, possibility signifying compensation for diminished basal ganglia functioning (Paulsen et al., 2004; Zimbelman et al., 2007). In contrast, we predicted hypoactivation of inhibitory networks for individuals with a high probability of diagnosis owing to a decline in corticostriatal functioning in individuals closer to a diagnosis. Since the functionality of brain systems in prHD may partially depend on the structural integrity of tissue, we also compared subcortical gray-matter volume and cortical volume and thickness in the control and prHD groups.

2. Materials and methods

2.1. Participants

The study sample consisted of 65 prHD and 36 controls. Data were collected at two PREDICT-HD sites, University of Iowa and Cleveland Clinic. Procedures were approved by the ethics committees at both sites and the study was performed in accordance with ethical guidelines in the 1964 Declaration of Helsinki. All participants provided written informed consent. Participants completed genetic testing for the CAG expansion prior to and independent from entry into PREDICT-HD. Confirmatory DNA testing was conducted on all study participants by PREDICT-HD. A certified examiner performed the Unified Huntington's Disease Rating Scale (UHDRS) (HSG, 1996) which contains 31 items that assess chorea, bradykinesia, rigidity, dystonia, and oculomotor function using a four-point scale (0 = normal; 4 = greatest impairment). The total motor score (TMS) is the sum of these items. On a subsequent item – the five-point Diagnostic Confidence Level – examiners rated their confidence level that participant's signs were an indication of HD. Participants were excluded if they had DCL = 4 (≥99% confidence of unequivocal signs of HD) at the time of entry into the current study. Additional exclusion criteria included clinical evidence of unstable medical or psychiatric illness, alcohol or drug abuse within the past year, learning or developmental disability requiring special education, history of another neurological condition, or an inability to undergo MRI scanning. Individuals were also excluded from participation if they had used prescription antipsychotic medications within the past six months or if they used phenothiazine-derivative antiemetic medications more than three times per month, but no other prescription or over-the-counter medications or natural remedies were restricted. All participants underwent comprehensive baseline evaluations including blood draw, neurological/motor examination, cognitive assessment, psychiatric and psychological questionnaires, and brain MRI.

The 65 prHD participants with the HD mutation were stratified into three groups based on their CAP score using the methods developed by Zhang et al. (2011) for PREDICT-HD. The CAP score is computed as CAP = (Age at scan) × (CAG – 33.66), and is very similar to the "burden score" of Penney, Vonsattel, MacDonald, Gusella, and Myers (1997). CAP scores can be converted to a scaled score (CAPs) based on a 5-year probability of diagnosis. Cut-offs for the three CAP groups (LOW, MEDIUM, and HIGH) were based on an optimization algorithm using the PREDICT-HD participants in the larger cohort (N > 1,000). The LOW group comprised CAPs scores <.67, the MEDIUM group between .67 and .85, and the HIGH group >.85. Based on this stratification the estimated time to diagnosis for each CAP group is > 12.78 years for the LOW group, between 12.78 and 7.59 for the MEDIUM group, and <7.59 years for the HIGH group. The study sample contained 21 LOW, 28 MEDIUM, and 16 HIGH prHD participants. The 36 control participants consisted of individuals who had a parent with HD, but who did not have the expanded CAG gene for HD (NEGATIVE group). The proportion of participants scanned at the Cleveland Clinic and University of Iowa was roughly equivalent across groups (Table 1).

Demographic and clinical variables for each sub-group are shown in Table 1. The decision to stratify the prHD participants into three subgroups rather than treat CAP score as a continuous variable was based on the need to compare the NEG and LOW groups to gain a better understanding of the very earliest functional brain changes in prHD. Comparing all the prHD participants with the NEG group would obscure these early changes. However, post-hoc correlations of CAP scores with MR signal intensity in regions of interest were also conducted (see below).

2.2. Executive function tests

All participants were administered three standardized executive function tasks outside the scanner: Stroop Color-Word Interference task (Golden & Freshwater, 2002), Symbol Digit Modalities Task (SDMT) (Smith, 1991), and Trails A and B (Reitan, 1958).

2.3. Stop signal fMRI task

The SST paradigm was similar to that described by Aron and Poldrack (2006) and is illustrated in Fig. 1. An advantage of the SST for fMRI experiments is that mechanisms of successful and unsuccessful inhibitory control can be examined since the thresholding method results in roughly equal numbers of correct and incorrect inhibitions. The SST consisted of 96 GO (75%) and 32 STOP (25%) trials distributed over 2 imaging runs. On all trials, the participant was presented with a 500 msec warning stimulus consisting of a central fixation cross. This was followed by a left or right arrow. For the GO trials, the participant responded as fast as possible with a left or right key press using the index and middle fingers of the right hand. For the STOP trials, a pure tone (900 Hz; duration, 500 msec) was presented subsequent to the GO (arrow) stimulus. The participant was instructed to attempt to stop his/her response at the appearance of the tone. The time between the GO (arrows) and STOP (tone) stimuli is referred to as the stop signal duration (SSD). The number of left and right arrows was equal; GO and STOP trials and left/right arrows were presented in a pseudorandom order.

The SSD on STOP trials changed depending on the participant's behavior. If the participant inhibited successfully on a STOP trial, then inhibition was made more difficult on a subsequent STOP trial by increasing the SSD by 50 msec; if the participant did not successfully inhibit, then inhibition was made easier by decreasing the SSD by 50 msec. Four staircases were used to ensure that the probability of correct inhibition (CI) was approximately 50% on trials at the end of the experiment. The four staircases started with SSD values of 100, 150, 200, and 250 msec respectively. Average SSD was computed, for each subject, from the values of the four staircases after the subject had converged on 50% correct inhibitions. Values for the last 12 moves of each staircase were averaged to give a stable SSD estimate. The stop signal reaction time (SSRT) was calculated by subtracting the final SSD from the mean of median RT on GO trials. Higher SSRT values are indicative of poorer inhibition. Therefore, higher values for the SSD indicate better inhibitory control. The task was programmed using Presentation software (Neurobehavioral Systems, Inc.) and displayed in the scanner using an Avotec back-projection video and audio systems (Avotec, Inc.).

2.4. MRI acquisition

MR data were acquired at two imaging sites: Cleveland Clinic and University of Iowa. Both sites used identical Siemens TIM Trio 3T MRI scanners (Erlangen, Germany) equipped with a 12-channel receive-only head array. To facilitate combining data across sites, experienced MR physicists (M.J.L., V.A.M.) set up and tested identical MRI protocols at both sites. Comparison of acquired phantom data indicated similar image quality and signal-to-noise ratio. Frequent QA scans were performed at each institution to ensure that imaging data were free of scanner artifacts and were comparable across scanner sites. Site comparability was also established by having 12 young healthy volunteers perform the SST at both sites in counter-balanced order; voxel-wise analyses performed on activation maps derived from each site did not demonstrate any differences in brain activation.

Whole-brain fMRI scans were acquired with a gradient-echo, echoplanar pulse sequence [31.4-mm thick contiguous axial slices, TE = 29 msec; TR = 2800 msec; flip angle = 80°; FOV = 256 × 256 mm; matrix = 128 × 128; in-plane resolution = 2 × 2 mm]. The SST task was performed over two imaging runs each lasting a total of 560 (200 volumes per imaging run). High resolution structural MRI (sMRI) scans [T1 with T1-weighted inversion recovery turboflash (MPRAGE), GRAPPA factor = 2,240 coronal slices, thickness = 1 mm, field of-view (FOV) = 256 mm × 256 mm, TI/TE/TR/flip angle (FA) = 900 msec/3.09 msec/2530 msec/10, matrix = 256 × 128, receiver bandwidth (BW) = 220 Hz/pixel] were acquired for registration with lower resolution EPI images and to measure cortical and subcortical gray- and white-matter volumes.

2.5. Image analysis (fMRI)

The first 4 pre-steady-state volumes of the EPI time series were removed. The remaining images were time shifted, motion corrected, and spatially filtered using a 2D 4 mm FWHM Gaussian filter in the Fourier domain. Multiple regression was performed using Analysis of Functional Neuroimaging (AFNI) software (Cox, 1996). A gamma variate HRF model used regressors for four trial types: GO correct (GO), GO incorrect, CI, and incorrect inhibition

(II). GO incorrect trials were not subsequently analyzed due to their low frequency (see Results). Individual subject t-maps for GO, CI and II trial types were converted to z-maps and transformed to Talairach stereotaxic space (Talairach & Tournoux, 1988).

Three t-test subtraction maps (CI > GO, II > GO, and II > CI) were generated for each of the 4 groups (NEGATIVE, LOW, MEDIUM, HIGH). A significant cluster was defined by an individual voxel probability ($p < .001$) and a minimum cluster size (.2 ml); these joint thresholds set the whole brain false-positive rate for a significant cluster equal to $p = .044$. A disjunction mask was then created for each contrast by combining all suprathreshold voxels from any of the four group t-maps. This produced functional ROI (fROI) maps for each of the three subtraction conditions. Large fROIs were divided along local minima in the averaged t-maps. Within each fROI and condition, z-statistics were averaged for each subject. For each fROI and subtraction condition, one-way ANCOVAS were conducted on the 4 groups to test for the main effect of group, adjusting for age. The false discovery rate (FDR) was used to correct for multiple comparisons. For those fROIs surviving the FDR correction, ANCOVAs were conducted to identify pairwise group differences in the magnitude of the fMRI response, adjusting for age. To determine if the degree of genetic exposure correlated with MR signal intensity in each fROI, post-hoc partial correlations of CAP scores with MR signal intensity (age adjusted) were also conducted.

2.6. Image analysis (sMRI)

Since structural brain changes could potentially alter brain functioning, structural MRI scans were analyzed to examine group differences in regional cortical volume and thickness as well as subcortical volumes. Cortical volume and thickness were derived from the Desikan atlas parcellation method incorporated in FreeSurfer 5.1 software (Fischl et al., 2004), which demonstrates good test-retest reliability across scanners and sites (Han et al., 2006; Reuter, Schmansky, Rosas, & Fischl, 2012). Each subject's MRI was initially analyzed in original space using the following analysis pipeline. Processing included removal of non-brain tissue by a hybrid water-shed/surface deformation procedure, subcortical structures were segmented (Fischl et al., 2002), and further intensity normalization was conducted. This was followed by white-matter segmentation, tessellation of the gray–white matter boundary, and automated topology correction (Fischl, Liu, & Dale, 2001). Then surface deformation following intensity gradients optimally placed the gray/white and gray/cerebro-spinal fluid borders at the location where the greatest shift in intensity defines the transition to the other tissue class (Fischl et al., 2001). Once the cortical models were complete, deformable procedures performed additional data processing and analysis, including parcellation of the cerebral cortex into 34 conventional gyral- and sulcal-based neuroanatomical regions in each hemisphere based on the Desikan atlas (Desikan et al., 2006). This parcellation method demonstrates diagnostic sensitivity in prHD (Harrington et al., 2014) and in other diseases (Desikan et al., 2009). Intensity and continuity information from the segmentation and deformation procedures produced representations of cortical thickness, which were calculated as the closest distance from the gray–white matter boundary to the gray-CSF boundary at each vertex on the tessellated surface (Fischl & Dale, 2000). FreeSurfer also outputs subcortical volumetric measures of the caudate, putamen, pallidum, nucleus accumbens, amygdala, hippocampus, thalamus, and cerebellum of each hemisphere.

Regional volumes were adjusted for total intracranial volume (ICV) by dividing each structure by ICV and multiplying by 100. One-way ANCOVAS testing for the main effect of group (4 groups), adjusting for age, were conducted on each of the 64 cortical thickness measures, 64 cortical thickness measures, and the 16 subcortical volume measures. The FDR correction for multiple comparisons was applied separately to the 34 left and 34 right hemisphere cortical regions, separately for cortical thickness and cortical volume, and to the 16 subcortical volumes (left and right hemisphere combined). For those volumes surviving the FDR correction, ANCOVAs, adjusted for age, were conducted for post-hoc pairwise group comparisons. Regional volumes that demonstrated significant changes in thickness or atrophy were then correlated with the SST measures and the fROI, in which group differences were identified.

We also calculated cortical thickness for fROIs using a FreeSurfer software routine designed to extract cortical thickness values from a ROI defined in volume space (http://surfer.nmr.mgh.harvard.edu/fswiki/VolumeRoiCorticalThickness). This was conducted for the 10 fROIs on the cortical surface. This was followed by a reanalysis of the fMRI group tests using ANCOVA with both age and cortical thickness as covariates.

3. Results

3.1. Demographic and clinical data

Group comparisons (Table 1) on continuous demographic variables and the UHDRS were conducted using an ANOVA, followed by post-hoc pairwise t-tests. The proportion of males, participants scanned at the Cleveland Clinic, and participants taking selective serotonin reuptake inhibitors (SSRI) medications were evaluated using the chi-square test. As expected, the NEGATIVE group was significantly older than the MEDIUM and LOW groups, and the HIGH group was also older than the LOW group (Table 1). There were no significant group differences in gender or education. The UHDRS TMS of the HIGH group was significantly greater than that of the NEGATIVE, LOW, and MEDIUM groups. The proportion of participants taking SSRI medications did not differ significantly across the four groups.

3.2. Executive function tests

Tests for group differences in executive function (Table 1) were conducted using an ANCOVA with age as a covariate, followed by post-hoc pairwise group ANCOVAs. No statistically significant group differences were observed on the SDMT. On the Stroop task, the NEGATIVE and LOW groups performed better than the HIGH group on color naming and the NEGATIVE and LOW groups performed better than the MEDIUM group, who in turn performed better than the HIGH group, on word reading (Table 1). The NEGATIVE and LOW groups performed better than the HIGH group on the Stroop Interference condition. On Trails A, B, and B-A, the NEGATIVE, LOW, and MEDIUM groups all performed significantly better than the HIGH group.

3.3. SST performance

Table 2 summarizes performance on the SST. As expected, performance exceeded 90% correct on the two-choice reaction time trials in the GO condition. STOP trials were evenly divided between correct and incorrect inhibitions, indicating the psychophysical staircases were operating as designed. ANCOVA (adjusting for age) failed to find significant group differences on any of the SST performance variables. However, it was notable that the SSD and SSRT were about 9% shorter/longer in the HIGH group compared to the NEGATIVE group, suggesting a trend for inhibitory control difficulties as individuals approached diagnosis. Because statistical power might have been lost in using CAP as a grouping variable, we therefore treated CAP as a continuous variable in a follow-up analysis. Partial correlations adjusting for age showed that CAP scores negatively correlated with the SSD ($r_{\text{partial}} = -.27$, $p < .05$), indicating that inhibitory control significantly declined as genetic exposure increased. No relationship was found between CAP scores and SSRT.

3.4. fMRI

The disjunction analysis identified 12 fROIs for the CI > GO subtraction, 11 fROIs for the II > GO subtraction, and 17 fROIs for the II > CI subtraction (Fig. 2). ANCOVAs tested for group differences in MRI signal intensity in each of these fROIs. Of these fROIs, significant group differences (i.e., FDR corrected) were found for two fROIs for the CI > GO, 5 fROIs for the II > GO, and 5 fROIs for the II > CI comparisons. These 12 fROIs are displayed in Fig. 3 and described in Table 3, which also reports the results from the post-hoc pairwise group ANCOVAs and the partial correlations of CAP scores with MR signal intensity, adjusted for age. Fig. 4 displays bar graphs of MRI signal in each of the 12 fROIs for the four groups.

For CI > GO comparison, all prHD groups demonstrated significant hypoactivation of the left angular gyrus/supra-marginal gyrus (SMG) relative to the negative group (fROI #1). Consistent with this finding, CAP scores did not correlate with left angular gyrus/SMG activation (Table 3). In contrast, only the HIGH group demonstrated significant hypoactivation of the right superior/middle temporal gyrus (MTG) (fROI #2). There was a nonsignificant trend for the LOW group to show hyperactivation in this region relative to the NEGATIVE group (η_p^2 [partial eta-squared] = .076; Fig. 4). Moreover, lower signal intensity in the right superior temporal gyrus (STG)/MTG also significantly correlated with higher CAP scores (Table 3).

For the II > GO comparison, only the HIGH group showed significant hypoactivation of the bilateral insula/IFG (fROIs #3 and #6) and bilateral angular gyrus/SMG (fROIs #4 and #5). For all of these fROIs, lower signal intensity was associated with higher CAP scores, indicating reductions in activation as genetic exposure increased. In contrast, the LOW group showed significant hyperactivation of the right SMA/anterior cingulate cortex (ACC) (fROI #7), and there was a nonsignificant trend for the HIGH group to show hypoactivation relative to the NEGATIVE group $\left(\eta_p^2 = .065\right)$. These results were consistent with the finding that lower signal intensity in the right SMA/ ACC correlated with higher CAP scores (Table 3).

The difference in activation between inhibition failures and successes (II > CI), was also typically attenuated in all prHD groups relative to the NEGATIVE group in most fROIs (except #10) (Fig. 4), although not always significantly. This finding was particularly striking in the left cerebellum (fROI #11), wherein significant hypoactivation was found in all prHD groups (Table 3, Fig. 4). Activation in the right PMC/postcentral gyrus (fROI #8) and the right insula (fROI #9) was also markedly reduced in the LOW and MEDIUM groups, and there were nonsignificant trends for reduced activation in the HIGH group relative to the NEGATIVE group $\left(\eta_p^2 = .051\right)$ and .065, respectively). Similarly, significant hypoactivation of the right brainstem (fROI #12) was found in the LOW and HIGH groups, with a nonsignificant trend for hypoactivation in the MEDIUM group relative $\left(\eta_p^2 = .045\right)$. Moreover, MR signal intensity in all of these fROIs did not significantly correlate with CAP scores, consistent with the general pattern of diminished differences between inhibition failures and successes, irrespective of genetic exposure (Fig. 4). One notable exception to this pattern of results was the right IFG (fROI #10), wherein the MEDIUM group showed hyperactivation relative to the NEGATIVE, LOW, and HIGH groups (Fig. 4).

The 10 cortical fROIs (#1–10) were reanalyzed using both age and cortical thickness as covariates to determine if the fMRI group differences were being driven by structural brain changes. All 10 fMRI ANCOVAs remained significant after FDR correction. Furthermore, none of the cortical thickness covariates were significantly associated with MR signal change in the 10 fROIs (p > .05, uncorrected).

3.4.1. Correlation of SST performance and fROIs—Given the significant correlation between SSD performance and CAP scores, partial correlations (age adjusted) were conducted to identify relationships between SSD and MRI signal intensity in the 12 fROIs, separately for the NEGATIVE and prHD groups. SSD significantly correlated with left angular gyrus (fROI #1) activation on correctly inhibited trials in both the NEGATIVE ($r_{partial}$ = .46, p = .005, uncorrected) and prHD groups ($r_{partial}$ = .27, p = .03, uncorrected), showing that better inhibitory control was associated with greater activation. The magnitude of this relationship did not differ significantly between the groups (t < 1.0). In the prHD group only, SSD also correlated with right PMC/postcentral gyrus activation (fROI #8; $r_{partial}$ = .27, p = .03, uncorrected), indicating that better inhibitory control also associated with greater ipsilateral sensorimotor activation for inhibition failures relative to successes.

3.5. sMRI

Results from ANCOVAs (age adjusted) testing group differences in cortical thickness, cortical volumes, and subcortical volumes are summarized in Supplementary Tables 1, 2 and 3, respectively. Six regions in the left hemisphere and four regions in the right hemisphere demonstrated significant group differences (p < .05, uncorrected) in cortical thickness (Supplementary Table 1); none of these 10 regions, however, survived an FDR correction for multiple comparisons. No cortical volumes (Supplementary Table 2) demonstrated significant group differences (p > .05, uncorrected). Seven of 16 subcortical regions demonstrated significant group differences after FDR correction for multiple comparisons, including the bilateral putamen, caudate and globus pallidus and the right nucleus

accumbens. Post-hoc ANCOVAs revealed that in all 7 regions the MEDIUM and HIGH groups showed significant tissue loss relative to the NEGATIVE group. In the LOW group, no volume loss was seen, but unexpectedly, there was a slight increase in right putamen volume relative to the NEGATIVE group.

3.5.1. Correlation of subcortical atrophy with fROIs and SSD performance—To determine if subcortical atrophy was related to functional changes in the brain in prHD, we correlated the basal ganglia and nucleus accumbens volumes with each fROI, adjusting for age. When inhibition failed (II > GO), MRI signal intensity in the right SMA/ACC (fROI #7) and the right insula/IFG (fROI #6) positively correlated with left globus pallidus volume ($r_{partial}$ = .43, p < .001 and $r_{partial}$ = .40, p < .001, respectively; FDR corrected). None of the other correlations reached statistical significance. The volumes of the basal ganglia and the right nucleus accumbens did not correlate with SSD performance in the prHD participants (p > .35, uncorrected).

4. Discussion

The present study is the first to uncover the specific cortical sources of response inhibition dysfunction in prHD. Though abnormal brain activation was predominantly observed when response inhibition failed, regionally circumscribed changes in brain functioning were also found when inhibition was successful. Changes in brain functioning were typically characterized by reductions in activation as estimated proximity to diagnosis neared, consistent with the finding that greater genetic exposure (higher CAP scores) significantly correlated with worse inhibitory control (SSD) and diminished activation of regions associated with successful (right STG/ MTG) and unsuccessful response inhibition (all fROIs). Yet in some regions hyperactivation was found in the LOW and the MEDIUM groups relative to controls, possibly signifying compensation. The results were not related to structural changes in grey-matter volume or thickness, or functional changes in visual centers, which exhibited normal activation in prHD.

When inhibitory control was successful, activation was remarkably normal in classic frontal inhibitory-centers including the bilateral IFG (BA 44, 45) and the medial-frontal cortices (Aron, 2011; Congdon et al., 2010; Levy & Wagner, 2011; Rubia et al., 2001), wherein activation was greater for CI than Go trials, but in all groups (Fig. 2). This finding contrasts with reports of abnormal FCz N2 (Beste et al., 2011) or P3 (Beste et al., 2010) amplitudes in prHD on correctly inhibited trials in a Go-NoGo task. While this result might suggest abnormal functioning of response inhibition or error monitoring networks, the findings are difficult to interpret since inhibition failures were not analyzed, owing to their infrequency in Go-NoGo tasks. Rather, the present study found that when inhibition was successful, activation was altered in prHD only in elements of the posterior ventral attention network (Corbetta, Patel, & Shulman, 2008), namely the left angular gyrus/SMG and the right STG/ MTG, the latter of which showed reductions in activation as individuals approached diagnosis. The ventral attention network is thought to be under stimulus-driven control as it responds to abrupt changes in events, such as those required during the SST. Thus, the network may facilitate response inhibition by reorienting attention to the stop signal (Congdon et al., 2010; Zhang & Li, 2012), which is compatible with the finding that left

SMG activation is selective to preparing to stop a response, but not implementing stopping (Majid et al., 2013). In the present study, better inhibitory control (SSD) on successfully inhibited trials correlated with greater left angular gyrus/SMG activation in the prHD and the control groups, possibly due to its role in 'motor' attention (Rushworth, Krams, & Passingham, 2001). Importantly, altered functioning in this region was detected early, with both the LOW and MEDIUM groups showing significant hypoactivation relative to controls.

Despite the finding that inhibition failures and successes produced greater activation than Go trials in similar systems (Fig. 2), response inhibition failures in prHD were related to changes in more distributed brain networks that govern inhibitory control, attention reorienting, and motor control. Moreover, reduced activation in two of these systems, namely inhibition and attention networks, was associated with greater genetic exposure. This finding underscores the importance of studying the basis of failed inhibition, unlike previous studies. Functioning was notably altered in frontal inhibition-centers including the bilateral IFG/insula and the right SMA/ACC (Aron et al., 2003; Aron & Poldrack, 2006; Li et al., 2006), which signal the basal ganglia to suppress a motor response via projections to the subthalamic nucleus (Aron, 2011; Congdon et al., 2010; Levy & Wagner, 2011; Majid et al., 2013; Rubia et al., 2001). The LOW group exhibited significant hyperactivation of the SMA/ACC, whereas the HIGH group exhibited striking hypoactivation of this network, possibly due in part to atrophy of the left globus pallidus, which correlated with greater hypoactivation of the right IFG/ insula and SMA/ACC. Though abnormal ERP FCz recordings might also suggest that SMA/ACC dysfunction in prHD is related to response inhibition (Beste et al., 2011), our findings demonstrate that altered activation of this region is specific to response inhibition failures, rather than reorienting attention to a NoGo signal, irrespective of inhibition success. Interestingly, prHD individuals close to a manifest diagnosis demonstrated hypoactivation of this inhibitory network when timing movements (Zimbelman et al., 2007), which also depends on inhibitory control (Merchant, Harrington, & Meck, 2013).

Response inhibition failures were also associated with dysfunction in components of the ventral attention network. In the HIGH group, we observed prominent hypoactivation of the bilateral inferior parietal cortex, including the right temporal-parietal junction (fROI #5), which mediates the detection of unexpected or infrequent events (Corbetta & Shulman, 2002), which is required on stop trials (Congdon et al., 2010). In addition, the LOW and MEDIUM groups, but also the HIGH group (medium effect size), showed little or no difference in activation of the right insula during inhibition failures than during successes (fROI #9), in striking contrast to the control group. This finding may suggest an early weakening in attentional monitoring of task-relevant signals by the insula (Menon & Uddin, 2010).

Differences in brain activation between failed and successful inhibitions also revealed abnormalities in ipsilateral motor-control networks, which are known to mediate the control of hand movements (Chiou et al., 2013; Derosiere et al., 2014). In the control group, activation was greater for inhibition failures than successes in the right sensori-motor cortex, left cerebellum, and right brainstem. This effect was markedly attenuated in all prHD groups in various fROIs, especially the cerebellum and brainstem, possibly indicating reduced

corticospinal excitability when inhibition failed. One speculation is that striatal dysfunction in prHD alters fast adjustments to movement-relevant goals, partly by disrupting communication with the cerebellum and brainstem, as it does in Parkinson's disease (Hacker, Perlmutter, Criswell, Ances, & Snyder, 2012; Jech, Mueller, Schroeter, & Ruzicka, 2013). In addition, ipsilateral sensorimotor activation differences between inhibition failures and successes were more attenuated as inhibitory control (SSD) in prHD worsened, further suggesting that altered ipsilateral motor-control network functioning contributed to deficient inhibitory control. This too may relate to a diminished capacity of the motor system to rapidly adjust for changes in movement goals, irrespective of genetic exposure.

An intriguing finding was the hyperactivation identified in the LOW group in a right hemisphere inhibitory center, namely the SMA/ACC (Levy & Wagner, 2011). This is of interest because in an fMRI study of motor timing (Zimbelman et al., 2007), hyperactivation of motor-control systems in individuals far from diagnosis was a key measure that distinguished controls and prHD groups in different prodromal stages. Another sign of potential compensation in response-inhibition centers was found in the MEDIUM group, which showed greater right IFG (BA 45) activation for inhibition failures than successes. Hyperactivation could be an intermediate phenotype of cell dysfunction, which begins long before cell death (Tobin & Signer, 2000). This presumed compensatory response may weaken as the neurodegenerative process advances. Indeed, a nonlinear trajectory of activation across the continuum of cognitive impairment (i.e., increases and decreases in brain activation) has been observed for mild cognitive impairment and Alzheimer's disease (Celone et al., 2006). Another possibility is that hyperactivation may be an early sign of dedifferentiation. To tease apart these explanations, longitudinal studies are needed that relate brain-activation to SST performance.

Altogether, our results suggest that response-inhibition failure in prHD is associated with functional changes in inhibitory control, attentional reorienting, and motor-control systems. Moreover, gradual reductions in activation of inhibitory control and attention systems were associated with greater genetic exposure, whereas the motor-control system exhibited a diminished capacity to flexibly adjust for changes in movement goals, irrespective of genetic exposure. Despite significant volume loss in various basal ganglia nuclei in the MEDIUM and HIGH groups, we did not find group differences in striatal activation. Volume loss in the basal ganglia nuclei also did not correlate with response inhibition capacity (SSD), which worsened with greater genetic exposure. Though we did not find significant cortical thinning and volume loss in the prHD group, our study may be underpowered in this respect, owing to reports of cortical thinning and volume loss in studies of large prHD samples (Harrington et al., 2014; Nopoulos et al., 2010). Nevertheless, we demonstrated that an fMRI probe of response inhibition capacity is more sensitive in identifying cortical dysfunction in prHD than contemporary structural MRI measures of gray-matter. This included the LOW group which showed significant changes in response inhibition, ventral attention, and motor-control centers. Our results strongly suggest that cortical dysfunction is an important source of response inhibition difficulties in prHD. A caveat is that hypoactivation of classic right-hemisphere inhibition centers (IFG/insula, SMA/ACC) appears partly related to globus pallidus atrophy, which was found only in the MEDIUM

and HIGH groups. Thus, as genetic exposure increases, structural changes in globus pallidus may also constrain functioning of the classic corticostriatal inhibitory control network.

Importantly, disease-related patterns of activation in the current study differ from those reported in prHD for other cognitive functions. For example, prHD individuals close to a diagnosis showed reduced right DLPFC and putamen activation during a phasic alerting task (Wolf et al., 2012) and reduced left DLPFC, but increased left inferior parietal activation during verbal working memory (Wolf et al., 2007). In contrast, basal ganglia activation declined with proximity to diagnosis during time discrimination (Paulsen et al., 2004), but was hyperactive during a set shifting task, irrespective of genetic exposure (Gray et al., 2013). These studies highlight the importance of assessing the functionality of brain circuits that govern different components of cognition in prHD, as they emphasize processing in different core brain circuits.

From a practical standpoint, the present results build upon emerging studies that are beginning to reveal early functional changes in brain circuits that govern different core cognitive functions, often in the absence of cognitive decline. Indeed, functional changes in several networks that govern response inhibition were found in the LOW group, despite no impairment on standard neuropsychological measures of executive functioning, including inhibitory control (Stroop Interference). Identification of the earliest functional changes in prHD is critical as this knowledge can be used to inform the preclinical stage at which interventions will be most efficacious and the selection of outcome measures that are more tailored to the treatment target. A notable strength of the current study is the large sample size, which enabled stratification of prHD participants based on estimated time to diagnosis and hence, adequate statistical power to identify the earliest signatures of changes in network functioning. Functional changes in brain circuits early in the disease process are often found in the absence of cortical or striatal volume loss, suggesting that functional biomarkers may be particularly sensitive to early neuropathology. Potential compensatory responses are especially intriguing, as they may be one of the earliest markers of neuropathology. Though our cross-sectional analyses suggested some stepwise changes in brain functioning from early to later stages of prHD, this prospect must be validated using longitudinal study designs. Of relevance here is that many cognitive measures are sensitive to changes in prHD in both cross-sectional and longitudinal studies (Paulsen, Smith, & Long, 2013). As such, functional imaging markers of cognitive change may well show longitudinal changes. Should the abnormalities in inhibitory control networks identified by the present study demonstrate longitudinal changes, it is conceivable that fMRI could be used as an outcome in trials aimed at slowing the disease prior to the appearance of atrophy and neuropsychological deficits. It will also be important to determine if the functionality of inhibitory control networks partly depends on microstructural changes in white-matter tissue (Matsui et al., 2014), which supports corticalecortical and corticostriatal communication. Clinical trials conducted during the prodromal stage of HD will likely require a combination of validated surrogate biomarkers, including functional and structural measures of the brain and neuropsychological measures that together may best evaluate novel treatments.

Supplementary Material

Refer to Web version on PubMed Central for supplementary material.

Acknowledgments

This work was supported by grants from the National Institute of Neurological Disorders and Stroke of the National Institutes of Health, (5RO1NS040068, 1U01NS082083, 5R01NS054893) and the CHDI Foundation. We thank the University of Iowa and Cleveland Clinic PREDICT-HD sites, the study participants, the National Research Roster for Huntington Disease Patients and Families, the Huntington's Disease Society of America and the Huntington Study Group. We acknowledge the assistance of Jeremy H. Bockholt. The content is solely the responsibility of the authors and does not necessarily represent the official views of the NIH.

REFERENCES

Andresen JM, Gayan J, Djousse L, Roberts S, Brocklebank D, Cherny SS, et al. The relationship between CAG repeat length and age of onset differs for Huntington's disease patients with juvenile onset or adult onset. Annals of Human Genetics. 2007; 71(Pt 3):295–301. http://dx.doi.org/10.1111/j.1469-1809.2006.00335.x. [PubMed: 17181545]

Aron AR. From reactive to proactive and selective control: developing a richer model for stopping inappropriate responses. Biological Psychiatry. 2011; 69:e55–e68. [PubMed: 20932513]

Aron AR, Poldrack RA. Cortical and subcortical contributions to stop signal response inhibition: role of the subthalamic nucleus. Journal of Neuroscience. 2006; 26(9):2424–2433. http://dx.doi.org/10.1523/JNEUROSCI.4682-05.2006. [PubMed: 16510720]

Aron AR, Schlaghecken F, Fletcher PC, Bullmore ET, Eimer M, Barker R, et al. Inhibition of subliminally primed responses is mediated by the caudate and thalamus: evidence from functional MRI and Huntington's disease. Brain : A Journal of Neurology. 2003; 126(Pt 3):713–723. [PubMed: 12566291]

Beste C, Ness V, Falkenstein M, Saft C. On the role of fronto-striatal neural synchronization processes for response inhibitioneevidence from ERP phase-synchronization analyses in pre-manifest Huntington's disease gene mutation carriers. Neuropsychologia. 2011; 49(12):3484–3493. http://dx.doi.org/10.1016/j.neuropsychologia.2011.08.024. [PubMed: 21906607]

Beste C, Saft C, Andrich J, Gold R, Falkenstein M. Response inhibition in Huntington's disease-a study using ERPs and sLORETA. Neuropsychologia. 2008; 46(5):1290–1297. http://dx.doi.org/10.1016/j.neuropsychologia.2007.12.008. [PubMed: 18241897]

Beste C, Willemssen R, Saft C, Falkenstein M. Response inhibition subprocesses and dopaminergic pathways: basal ganglia disease effects. Neuropsychologia. 2010; 48(2):366–373. http://dx.doi.org/10.1016/j.neuropsychologia.2009.09.023. [PubMed: 19782093]

Boehler CN, Appelbaum LG, Krebs RM, Hopf JM, Woldorff MG. Pinning down response inhibition in the braineconjunction analyses of the stop-signal task. NeuroImage. 2010; 52(4):1621–1632. http://dx.doi.org/10.1016/j.neuroimage.2010.04.276. [PubMed: 20452445]

Celone KA, Calhoun VD, Dickerson BC, Atri A, Chua EF, Miller SL, et al. Alterations in memory networks in mild cognitive impairment and Alzheimer's disease: an independent component analysis. Journal of Neuroscience. 2006; 26(40):10222–10231. http://dx.doi.org/10.1523/JNEUROSCI.2250-06.2006. pii: 26/40/10222. [PubMed: 17021177]

Chiou SY, Wang RY, Liao KK, Wu YT, Lu CF, Yang YR. Co-activation of primary motor cortex ipsilateral to muscles contracting in a unilateral motor task. Clinical Neurophysiology. 2013; 124:1353–1363. [PubMed: 23478202]

Congdon E, Mumford JA, Cohen JR, Galvan A, Aron AR, Xue G, et al. Engagement of large-scale networks is related to individual differences in inhibitory control. NeuroImage. 2010; 53(2):653–663. http://dx.doi.org/10.1016/j.neuroimage.2010.06.062. pii: S1053-8119(10)00920-1. [PubMed: 20600962]

Corbetta M, Patel G, Shulman GL. The reorienting system of the human brain: from environment to theory of mind. Neuron. 2008; 58(3):306–324. http://dx.doi.org/10.1016/j.neuron.2008.04.017. pii: S0896-6273(08)00369-3. [PubMed: 18466742]

Corbetta M, Shulman GL. Control of goal-directed and stimulus-driven attention in the brain. Nature Reviews Neuroscience. 2002; 3(3):201–215.

Cox RW. AFNI: software for analysis and visualization of functional magnetic resonance neuroimages. Computers and Biomedical Research, an International Journal. 1996; 29(3):162–173.

Derosiere G, Alexandre F, Bourdillon N, Mandrick K, Ward TE, Perrey S. Similar scaling of contralateral and ipsilateral cortical responses during graded unimanual force generation. NeuroImage. 2014; 85(Pt 1):471–477. [PubMed: 23416251]

Desikan RS, Cabral HJ, Hess CP, Dillon WP, Glastonbury CM, Weiner MW, et al. Alzheimer's Disease Neuroimaging, I. Automated MRI measures identify individuals with mild cognitive impairment and Alzheimer's disease. Brain. 2009; 132(Pt 8):2048–2057. http://dx.doi.org/10.1093/brain/awp123. [PubMed: 19460794]

Desikan RS, Segonne F, Fischl B, Quinn BT, Dickerson BC, Blacker D, et al. An automated labeling system for subdividing the human cerebral cortex on MRI scans into gyral based regions of interest. NeuroImage. 2006; 31(3):968–980. http://dx.doi.org/10.1016/j.neuroimage.2006.01.021. [PubMed: 16530430]

Duff K, Paulsen J, Mills J, Beglinger LJ, Moser DJ, Smith MM, et al. Mild cognitive impairment in prediagnosed Huntington disease. Neurology. 2010; 75(6):500–507. http://dx.doi.org/10.1212/WNL.0b013-3181eccfa2. [PubMed: 20610833]

Duyao M, Ambrose C, Myers R, Novelletto A, Persichetti F, Frontali M, et al. Trinucleotide repeat length instability and age of onset in Huntington's disease. Nature Genetics. 1993; 4(4):387–392. http://dx.doi.org/10.1038/ng0893-387. [PubMed: 8401587]

Fischl B, Dale AM. Measuring the thickness of the human cerebral cortex from magnetic resonance images. Proceedings of the National Academy of Sciences of the United States of America. 2000; 97(20):11050–11055. http://dx.doi.org/10.1073/pnas.200033797. [PubMed: 10984517]

Fischl B, van der Kouwe A, Destrieux C, Halgren E, Segonne F, Salat DH, et al. Automatically parcellating the human cerebral cortex. Cerebral Cortex. 2004; 14(1):11–22. [PubMed: 14654453]

Fischl B, Liu A, Dale AM. Automated manifold surgery: constructing geometrically accurate and topologically correct models of the human cerebral cortex. IEEE Transactions on Medical Imaging. 2001; 20(1):70–80. http://dx.doi.org/10.1109/42.906426. [PubMed: 11293693]

Fischl B, Salat DH, Busa E, Albert M, Dieterich M, Haselgrove C, et al. Whole brain segmentation: automated labeling of neuroanatomical structures in the human brain. Neuron. 2002; 33(3):341–355. [PubMed: 11832223]

Georgiou-Karistianis N, Farrow M, Wilson-Ching M, Churchyard A, Bradshaw JL, Sheppard DM. Deficits in selective attention in symptomatic Huntington disease: assessment using an attentional blink paradigm. Cognitive and Behavioral Neurology: Official Journal of the Society for Behavioral and Cognitive Neurology. 2012; 25(1):1–6. http://dx.doi.org/10.1097/WNN.0b013-318248c503. [PubMed: 22310306]

Golden, CJ.; Freshwater, SM. Stroop color and word test: Revised examiner's manual. Stoelting Co.; Wood Dale, IL: 2002.

Gray MA, Egan GF, Ando A, Churchyard A, Chua P, Stout JC, et al. Prefrontal activity in Huntington's disease reflects cognitive and neuropsychiatric disturbances: the IMAGE-HD study. Experimental Neurology. 2013; 239:218–228. http://dx.doi.org/10.1016/j.expneurol.2012.10.020. pii: S0014-4886(12)00403-7. [PubMed: 23123406]

Hacker CD, Perlmutter JS, Criswell SR, Ances BM, Snyder AZ. Resting state functional connectivity of the striatum in Parkinson's disease. Brain. 2012; 135(Pt 12):3699–3711. http://dx.doi.org/10.1093/brain/aws281. pii: aws281. [PubMed: 23195207]

Hampshire A, Chamberlain SR, Monti MM, Duncan J, Owen AM. The role of the right inferior frontal gyrus: inhibition and attentional control. NeuroImage. 2010; 50(3):1313–1319. http://dx.doi.org/10.1016/j.neuroimage.2009.12.109. [PubMed: 20056157]

Han X, Jovicich J, Salat D, van der Kouwe A, Quinn B, Czanner S, et al. Reliability of MRI-derived measurements of human cerebral cortical thickness: the effects of field strength, scanner upgrade and manufacturer. NeuroImage. 2006; 32(1):180–194. http://dx.doi.org/10.1016/j.neuroimage.2006.02.051. [PubMed: 16651008]

Harrington DL, Liu D, Smith MM, Mills JA, Long JD, Aylward EH, et al. Neuroanatomical correlates of cognitive functioning in prodromal Huntington disease. Brain and Behavior. 2014; 4(1):28–40. doi: 10.1002Jbrb3.18S.

Harrington DL, Smith MM, Zhang Y, Carlozzi NE, Paulsen JS. Cognitive domains that predict time to diagnosis in prodromal Huntington disease. Journal of Neurology, Neurosurgery, and Psychiatry. 2012; 83(6):612–619. http://dx.doi.org/10.1136/jnnp-2011-301732.

Henderson T, Georgiou-Karistianis N, White O, Millist L, Williams DR, Churchyard A, et al. Inhibitory control during smooth pursuit in Parkinson's disease and Huntington's disease. Movement Disorders: Official Journal of the Movement Disorder Society. 2011; 26(10):1893–1899. http://dx.doi.org/10.1002/mds.23757. [PubMed: 21630355]

HSG. Unified Huntington's disease rating scale: reliability and consistency. Movement Disorders. 1996; 11:136–142. [PubMed: 8684382]

Jech R, Mueller K, Schroeter ML, Ruzicka E. Levodopa increases functional connectivity in the cerebellum and brainstem in Parkinson's disease. Brain. 2013; 136:e234. [PubMed: 23370091]

Levy BJ, Wagner AD. Cognitive control and right ventrolateral prefrontal cortex: reflexive reorienting, motor inhibition, and action updating. Annals of the New York Academy of Sciences. 2011; 1224:40–62. http://dx.doi.org/10.1111/j.1749-6632.2011.05958.x. [PubMed: 21486295]

Li CS, Huang C, Constable RT, Sinha R. Imaging response inhibition in a stop-signal task: neural correlates independent of signal monitoring and post-response processing. The Journal of Neuroscience. 2006; 26:186–192. [PubMed: 16399686]

Majid DS, Cai W, Corey-Bloom J, Aron AR. Proactive selective response suppression is implemented via the basal ganglia. Journal of Neuroscience. 2013; 33(33):13259–13269. http://dx.doi.org/10.1523/JNEUROSCI.5651-12.2013. [PubMed: 23946385]

Matsui JT, Vaidya JG, Johnson HJ, Magnotta VA, Long JD, Mills JA, et al. Diffusion weighted imaging of prefrontal cortex in prodromal huntington's disease. Human Brain Mapping. 2014; 35:1562–1573. [PubMed: 23568433]

Menon V, Uddin LQ. Saliency, switching, attention and control: a network model of insula function. Brain Structure & Function. 2010; 214(5-6):655–667. http://dx.doi.org/10.1007/s00429-010-0262-0. [PubMed: 20512370]

Merchant H, Harrington DL, Meck WH. Neural basis of the perception and estimation of time. Annual Review of Neuroscience. 2013; 36

Nopoulos PC, Aylward EH, Ross CA, Johnson HJ, Magnotta VA, Juhl AR, et al. Cerebral cortex structure in prodromal Huntington disease. Neurobiology of Disease. 2010; 40(3):544–554. http://dx.doi.org/10.1016/j.nbd.2010.07.014. [PubMed: 20688164]

Novak MJ, Warren JD, Henley SM, Draganski B, Frackowiak RS, Tabrizi SJ. Altered brain mechanisms of emotion processing in pre-manifest Huntington's disease. Brain. 2012; 135(Pt 4):1165–1179. http://dx.doi.org/10.1093/brain/aws024. pii: aws024. [PubMed: 22505631]

O'Rourke JJ, Beglinger LJ, Smith MM, Mills J, Moser DJ, Rowe KC, et al. The trail making test in prodromal Huntington disease: contributions of disease progression to test performance. Journal of Clinical and Experimental Neuropsychology. 2011; 33(5):567–579. http://dx.doi.org/10.1080/13803395.2010.541228. [PubMed: 21302170]

Paulsen JS, Hayden M, Stout JC, Langbehn DR, Aylward E, Ross CA, et al. Predict H. D. I. o. t. H. S. G. Preparing for preventive clinical trials: the Predict-HD study. Archives of Neurology. 2006; 63(6):883–890. http://dx.doi.org/10.1001/archneur.63.6.883. [PubMed: 16769871]

Paulsen JS, Langbehn DR, Stout JC, Aylward E, Ross CA, Nance M, et al. Detection of Huntington's disease decades before diagnosis: the predict-HD study. Journal of Neurology, Neurosurgery & Psychiatry. 2008; 79(8):874–880. http://dx.doi.org/10.1136/jnnp.2007.128728.

Paulsen JS, Smith MM, Long JD. Cognitive decline in prodromal Huntington Disease: implications for clinical trials. Journal of Neurology, Neurosurgery & Psychiatry. 2013; 84(11):1233–1239.

Paulsen JS, Zhao H, Stout JC, Brinkman RR, Guttman M, Ross CA, et al. Huntington Study, G. Clinical markers of early disease in persons near onset of Huntington's disease. Neurology. 2001; 57(4):658–662. [PubMed: 11524475]

Paulsen JS, Zimbelman JL, Hinton SC, Langbehn DR, Leveroni CL, Benjamin ML, et al. fMRI biomarker of early neuronal dysfunction in presymptomatic Huntington's Disease. AJNR Am J Neuroradiol. 2004; 25(10):1715–1721. [PubMed: 15569736]

Penney JB Jr. Vonsattel JP, MacDonald ME, Gusella JF, Myers RH. CAG repeat number governs the development rate of pathology in Huntington's disease. Annals of Neurology. 1997; 41(5):689–692. http://dx.doi.org/10.1002/ana.410410521. [PubMed: 9153534]

Reading SA, Dziorny AC, Peroutka LA, Schreiber M, Gourley LM, Yallapragada V, et al. Functional brain changes in presymptomatic Huntington's disease. Annals of Neurology. 2004; 55(6):879–883. http://dx.doi.org/10.1002/ana.20121. [PubMed: 15174024]

Reitan RM. Validity of the trail making test as an indicator of organic brain damage. Perceptual and Motor Skills. 1958; 8:271–276.

Reuter M, Schmansky NJ, Rosas HD, Fischl B. Within-subject template estimation for unbiased longitudinal image analysis. NeuroImage. 2012; 61(4):1402–1418. http://dx.doi.org/10.1016/j.neuroimage.2012.02.084. [PubMed: 22430496]

Rosas HD, Hevelone ND, Zaleta AK, Greve DN, Salat DH, Fischl B. Regional cortical thinning in preclinical Huntington disease and its relationship to cognition. Neurology. 2005; 65(5):745–747. http://dx.doi.org/10.1212/01.wnl.0000174432.87383.87. [PubMed: 16157910]

Rubia K, Russell T, Overmeyer S, Brammer MJ, Bullmore ET, Sharma T, Simmons A, Williams SC, Giampietro V, Andrew CM, Taylor E. Mapping motor inhibition: conjunctive brain activations across different versions of go/no-go and stop tasks. Neuroimage. 2001; 13:250–261. [PubMed: 11162266]

Rushworth MF, Krams M, Passingham RE. The attentional role of the left parietal cortex: the distinct lateralization and localization of motor attention in the human brain. Journal of Cognitive Neuroscience. 2001; 13(5):698–710. [PubMed: 11506665]

Smith, A. Symbol digit modalities test. Western Psychological Services; Los Angeles, CA: 1991.

Stout JC, Paulsen JS, Queller S, Solomon AC, Whitlock KB, Campbell JC, et al. Neurocognitive signs in prodromal Huntington disease. Neuropsychology. 2011; 25(1):1–14. http://dx.doi.org/10.1037/a0020937. [PubMed: 20919768]

Swerdlow NR, Paulsen JS, Braff DL, Butters N, Geyer MA, Swenson MR. Impaired prepulse inhibition of acoustic and tactile startle response in patients with Huntington's disease. Journal of Neurology, Neurosurgery & Psychiatry. 1995; 58:192–200.

Talairach, J.; Tournoux, P. Co-planar stereotaxic atlas of the human brain. Thieme; New York: 1988.

Tobin AJ, Signer ER. Huntington's disease: the challenge for cell biologists. Human Brain Mapping. 2000; 10(12):531–536. pii: S0962-8924(00)01853-5.

Vonsattel JP, DiFiglia M. Huntington disease. Journal of Neuropathology and Experimental Neurology. 1998; 57(5):369–384. [PubMed: 9596408]

Wolf RC, Gron G, Sambataro F, Vasic N, Wolf ND, Thomann PA, et al. Brain activation and functional connectivity in premanifest Huntington's disease during states of intrinsic and phasic alertness. Human Brain Mapping. 2012; 33(9):2161–2173. http://dx.doi.org/10.1002/hbm.21348. [PubMed: 22887827]

Wolf RC, Sambataro F, Vasic N, Schonfeldt-Lecuona C, Ecker D, Landwehrmeyer B. Aberrant connectivity of lateral prefrontal networks in presymptomatic Huntington's disease. Experimental Neurology. 2008; 213(1):137–144. http://dx.doi.org/10.1016/j.expneurol.2008.05.017. [PubMed: 18588876]

Wolf RC, Vasic N, Schonfeldt-Lecuona C, Landwehrmeyer GB, Ecker D. Dorsolateral prefrontal cortex dysfunction in presymptomatic Huntington's disease: evidence from event-related fMRI. Brain: A Journal of Neurology. 2007; 130(Pt 11):2845–2857. http://dx.doi.org/10.1093/brain/awm210. [PubMed: 17855375]

Zhang S, Li CR. Functional networks for cognitive control in a stop signal task: independent component analysis. Human Brain Mapping. 2012; 33:89–104. [PubMed: 21365716]

Zhang Y, Long JD, Mills JA, Warner JH, Lu W, Paulsen JS. Indexing disease progression at study entry with individuals at-risk for Huntington disease. American Journal of Medical Genetics. Part B, Neuropsychiatric Genetics: The Official Publication of the International Society of Psychiatric Genetics. 2011; 156B(7):751–763. http://dx.doi.org/10.1002/ajmg.b.31232.

Zimbelman JL, Paulsen JS, Mikos A, Reynolds NC, Hoffmann RG, Rao SM. fMRI detection of early neural dysfunction in preclinical Huntington's disease. J Int Neuropsychol Soc. 2007; 13(5):758–769. http://dx.doi.org/10.1017/S1355617707071214. [PubMed: 17697407]

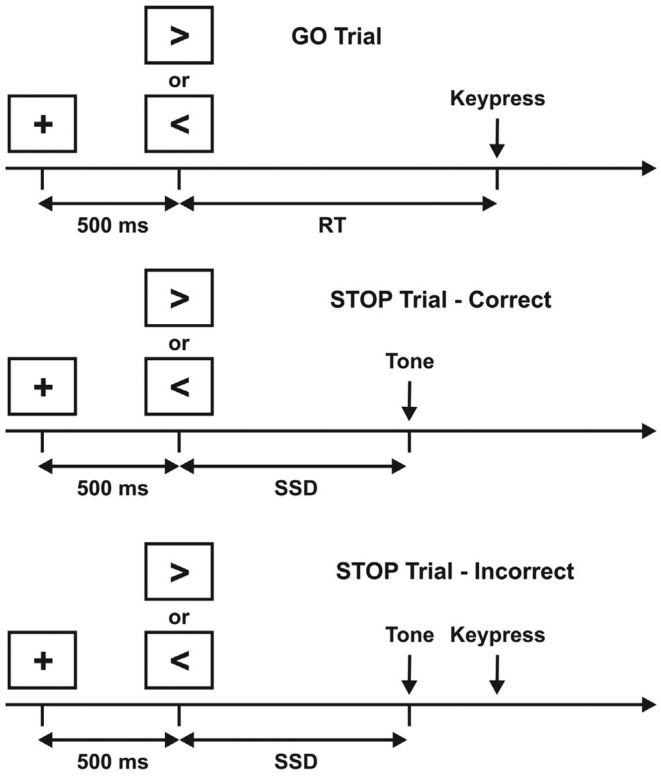

Fig. 1.
Schematic timeline for the stop signal task (see Methods for details).

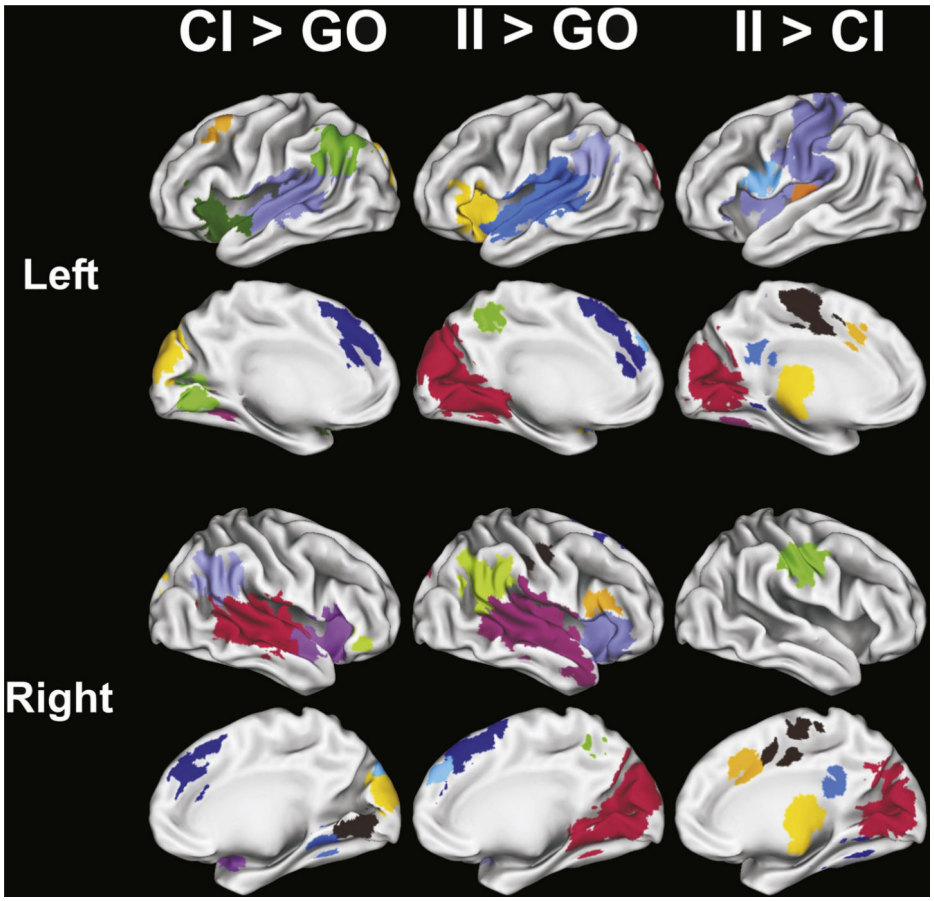

Fig. 2.

fROIs derived from the CI > GO (*N* = 12), II > GO (*N* = 11), and II > CI (*N* = 17) subtractions. CI = correct inhibition trials, II = incorrect inhibition trials, GO = go trials. Colors are used to demarcate the different fROIs and have no interpretive significance. Background gray-scale brain images derived from a rendering of the gray–white matter surface using Caret software (Washington University, St. Louis).

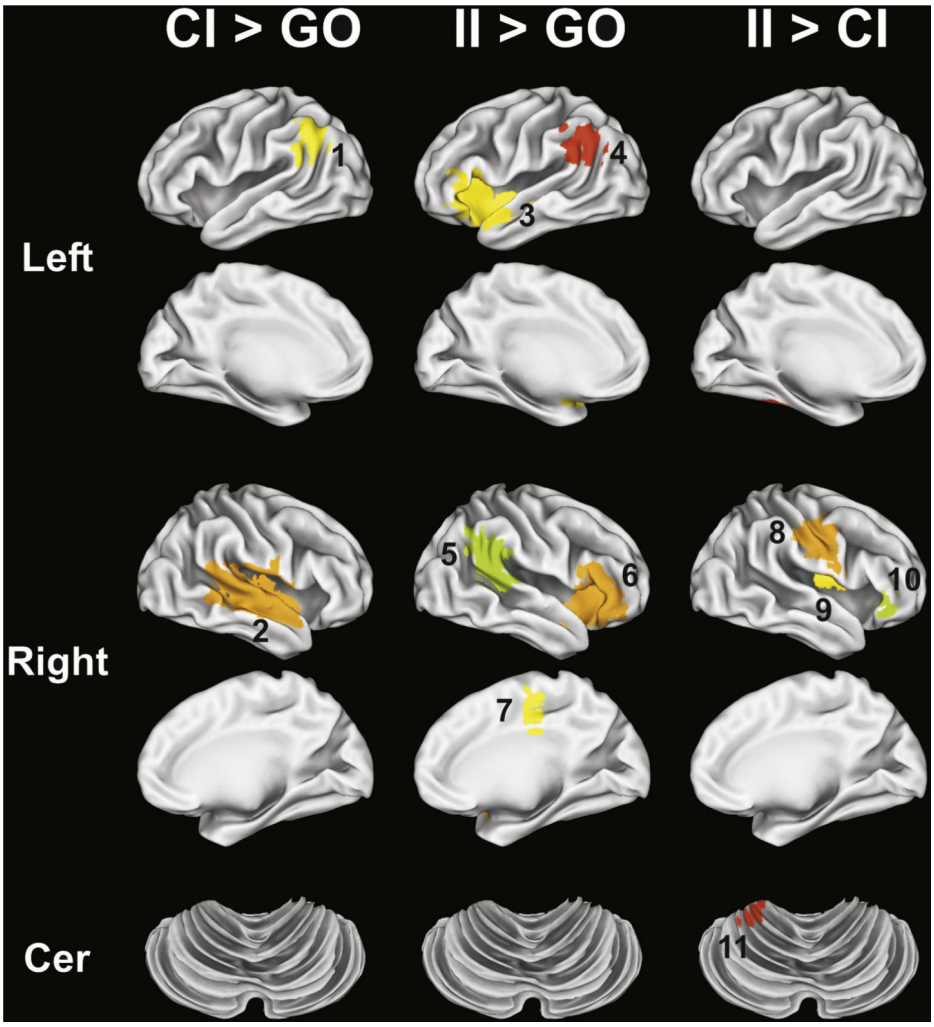

Fig. 3.

fROIs (shown in color) demonstrating significant group differences. fROI numbers correspond with region numbers in Table 3 and Fig. 4. CI = correct inhibition trials, II = incorrect inhibition trials, GO = go trials. Background gray-scale brain images derived from a rendering of the gray–white matter surface using Caret software (Washington University, St. Louis).

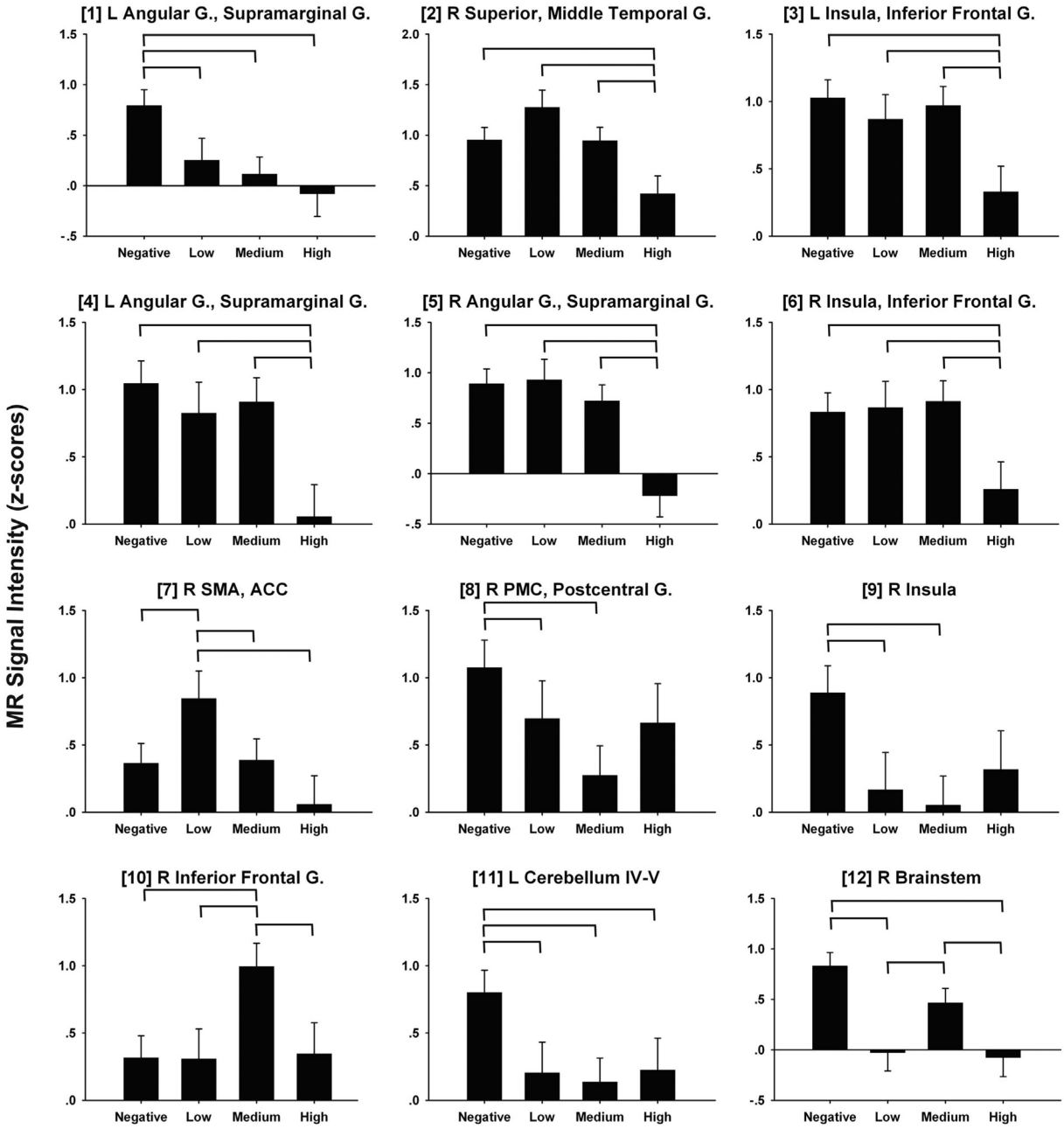

Fig. 4.

Bar graphs illustrating group differences in MR signal intensity for the CI > GO, II > GO, and II > CI subtractions. Age-adjusted group means and standard errors are plotted. Numbers in brackets correspond to fROI numbers in Table 3 and Fig. 3. Significant pairwise group differences are designated by horizontal bars and based on ANCOVA (age as covariate) post-hoc tests (Table 3). Note that fROIs #1–2 are from CI > GO subtraction, fROI #3–7 from II > GO, and fROI #8–12 from II > CI. MR signal intensity in z-scores. G = gyrus; R = right; L = left; B = bilateral; ACC = anterior cingulate cortex; SMA = supplementary motor area.

Table 1

Demographic, disease, and executive function variables for the NEGATIVE, LOW, MEDIUM, and HIGH groups.

	NEGATIVE	LOW	MEDIUM	HIGH	*p*	Posthocs
	***n* = 36**	***n* = 21**	***n* = 28**	***n* = 16**		
Demographic and disease variables						
Age – mean yrs. (SD; range)	49.2 (9.6; 24–62)*	31.6 (8.1; 19–49)	41.6 (12.6; 22–77)	45.3 (11.4; 27–68)	***<.001***	Neg > Med > Low; High > Low
Education – mean yrs. (SD; range)	15.5 (1.9; 12–20)	14.7 (2.3; 12–20)	15.2 (2.8; 11–19)	14.3 (3.1; 10–18)	.344	
Sex – no. male (%)	11 (31.4)	4 (19.0)	8 (28.6)	3 (18.8)	.660	
CAG repeat length – mean no. (SD)	20.1 (3.7)	41.9 (1.7)	42.3 (2.7)	43.9 (3.1)		
UHDRS Motor Score – mean (SD; range)	5.0 (3.9; 0–19)	3.2 (2.6; 0–10)	7.0 (6.6; 0–30)	12.3 (8.6; 1–29)	***<.001***	High > Neg, Low, Med
SSRI use – mean no. (%)	9 (25.7)	8 (38.1)	8 (28.6)	8 (50.0)	.330	
Location scanned (Cleveland Clinic/U. of Iowa)	14/22	9/12	15/13	8/8	.669	
Executive function test scores						
SDMT – mean no. correct (SD; range)	54.3 (9.7; 28–79)	57.2 (8.5; 39–72)	53.6 (10.8; 28–79)	48.4 (10.7; 32–64)	.070	
Stroop color – mean no. correct (SD; range)	84.7 (11.5; 63–115)	84.4 (9.7; 66–112)	80.3 (12.4; 60–116)	72.6 (16.1; 45–96)	***.009***	Neg, Low > High
Stroop word – mean no. correct (SD; range)	107.4 (17.2; 71–143)	107.5 (12.5; 88–141)	98.2 (16.4; 50–128)	83.6 (21.5; 50–113)	***<.001***	Neg, Low > Med > High
Stroop interference - mean no. correct (SD; range)	48.7 (8.9; 30–66)	52.2 (12.5; 24–76)	48.3 (12.4; 25–78)	41.1 (13.2; 24–76)	***.038***	Neg, Low > High
Trails A – mean secs (SD; range)	22.2 (7.1; 16–52)	20.7 (7.3; 11–38)	22.9 (7.7; 11–40)	28.9 (11.8; 16–64)	***.024***	Neg, Low, Med < High
Trails B – mean secs (SD; range)	53.9 (23.0; 32–146)	46.3 (14.9; 20–89)	54.6 (23.3; 29–132)	77.6 (35.7; 41–146)	***.002***	Neg, Low, Med < High
Trails B-A – mean secs (SD; range)	30.5 (20.5; 8–122)	25.5 (12.7; 7–59)	31.2 (19.7; 12–93)	48.0 (31.2; 13–115)	***.016***	Neg, Low, Med < High

Bolded and italicized *p*-values indicate statistical significance.

Higher executive function test scores signify better performance; the exception is the trails test, where lower scores signify better performance.

UHDRS = Unified Huntington's Disease Rating Scale; SSRI = selective serotonin reuptake inhibitors; SDMT = Symbol Digit Modalities Test.

Table 2

Stop signal task performance.

	NEGATIVE	LOW	MEDIUM	HIGH	*p*	η_p^2
GO Correct – mean % (SD; range)	94.2 (3.3; 86–99)	94.8 (3.7; 84–99)	92.6 (6.9; 68–99)	91.1 (7.8; 66–97)	NS	.055
GO Correct RT – mean of median msec (SD; range)	678.2 (68.9; 506–796)	635.7 (59.1; 510–745)	647.3 (75.9; 458–793)	641.8 (49.1; 525–731)	NS	.030
STOP Correct – mean % correct (SD; range)	51.0 (8.0; 30–67)	51.8 (7.4; 39–64)	51.2 (6.8; 39–67)	51.1 (9.3; 36–66)	NS	.009
SSD – mean msec (SD; range)	493.9 (97.5; 175–623)	451.3 (91.0; 246–596)	452.3 (102.8; 220–621)	433.1 (83.5; 271–550)	NS	.046
SSRT – mean msec (SD; range)	185.3 (48.7; 99–331)	180.5 (47.3; 115–315)	197.0 (52.3; 117–404)	205.5 (58.2; 151–401)	NS	.028

*Mean (SD).

RT = reaction time; SSD = stop signal duration; SSRT = stop signal reaction time (GO correct RT – SSD).

η_p^2 = partial eta-squared, a measure of effect size.

Table 3

fROIs demonstrating significant ($p < .05$, corrected) oneway ANCOVA group effects (age as covariate).

#	Side	Region	BA	Tailarach coordinates			Vol. (ml)	*p*	η_p^2	PostHoc	$r_{partial}$ (*p*)*
				x	*y*	*z*					
CI > GO											
1	L	Angular G., Supramarginal G.	7, 39, 40	–50	–53	34	1.8	.004	.125	Neg > Low, Med, High	
2	R	Superior, Middle Temporal G.	22	53	–23	4	17.3	.006	.112	Neg, Low, Med > High	–.323 (.009)
II > GO											
3	L	Insula, Inferior Frontal G.	44, 45	–37	14	1	10.5	.015	.097	Neg, Low, Med > High	–.266 (.033)
4	L	Angular G., Supramarginal G.	39, 40	–53	–49	28	2.2	.005	.116	Neg, Low, Med > High	–.334 (.007)
5	R	Angular G., Supramarginal G.	22, 39, 40	52	–47	23	3.4	<.001	.189	Neg, Low, Med > High	–.466 (.00009)
6	R	Insula, Inferior Frontal G.	44, 45	41	19	2	.4	.019	.074	Neg, Low, Med > High	–.261 (.035)
7	R	SMA, ACC	6, 24	6	–22	47	.4	.003	.068	Low > Neg, Med, High	–.302 (.015)
II > CI											
8	R	PMC, Postcentral G.	3, 4	49	–15	35	2.9	.010	.069	Neg > Low, Med	
9	R	Insula		36	–10	16	.2	.008	.082	Neg > Low, Med	
10	R	Inferior frontal G.	45	45	27	0	.3	.011	.102	Med > Neg, Low, High	
11	L	Cerebellum IV-V	–	–25	–38	–21	.2	.002	.085	Neg > Low, Med, High	
12	R	Brainstem	–	5	–32	–47	.4	<.001	.181	Neg, Med > Low, High	

CI > GO = subtraction of go correct from correct inhibition conditions; II > GO = subtraction of go correct from incorrect inhibition conditions; II > CI = subtraction of correct inhibition from incorrect inhibition conditions.

= numbers correspond to fROI regions in Figs. 3 and 4.

ACC = anterior cingulate cortex; IFG = inferior frontal gyrus; MTG = middle temporal gyrus; SMA = supplementary motor area; SMG = supramarginal gyrus; STG = superior temporal gyrus; BA = Brodmann Area; G – gyrus; R = right; L = left; B = bilateral.

η_p^2 = partial eta-squared, a measure of effect size.

* Significant ($p < .5$) partial correlations between CAP score and MR signal intensity, with age as a covariate.